Please cite the paper as follows:

De-Prada-Gil, M., Díaz-González, F., Gomis-Bellmunt, O., Sumper, A.
DFIG-based offshore wind power plant connected to a single VSC-HVDC operated at variable frequency: Energy yield assessment
(2015) Energy, 86, pp. 311-322.

DFIG–based offshore wind power plant connected to a single VSC–HVDC operated at variable frequency: Energy yield assessment

Mikel De-Prada-Gil[a,*], Francisco Díaz–González[a], Oriol Gomis-Bellmunt[a,b,c], Andreas Sumper[a,b,c]

[a] *IREC Catalonia Institute for Energy Research, Jardins de les Dones de Negre 1, 2a. 08930 Sant Adrià de Besòs, Barcelona (Spain).*
[b] *Centre d'Innovació Tecnològica en Convertidors Estàtics i Accionaments (CITCEA-UPC), Universitat Politècnica de Catalunya UPC, C. Comte d'Urgell, 187, Pl. 2. 08036 Barcelona, Spain*
[c] *Centre d'Innovació Tecnològica en Convertidors Estàtics i Accionaments (CITCEA-UPC), Universitat Politècnica de Catalunya UPC, Av. Diagonal, 647, Pl. 2. 08028 Barcelona, Spain*

Abstract

The existence of HVDC transmission systems for remote offshore wind power plants allows devising novel wind plant concepts, which do not need to be synchronized with the main AC grid. This paper proposes an offshore wind power plant (OWPP) design based on variable speed wind turbines driven by doubly fed induction generators (DFIGs) with reduced power electronic converters connected to a single VSC–HVDC converter which operates at variable frequency and voltage within the collection grid. It is aimed to evaluate the influence of the power converter size and wind speed variability within the WPP on energy yield efficiency, as well as to develop a coordinated control between the VSC–HVDC converter and the individual back–to–back reduced power converters of each DFIG–based wind turbine in order to provide control capability for the wind power plant at a reduced cost. To maximise wind power generation by the OWPP, an optimum electrical frequency search algorithm for the VSC–HVDC converter is proposed. Both central wind power plant control level and local wind turbine control level are presented and the performance of the system is

*Corresponding author
Email address: mdeprada@irec.cat. Jardins de les Dones de Negre 1, 2a. 08930 Sant Adrià de Besòs, Barcelona (Spain). Tel. +34 933562615 Fax. +34 933563802 (Mikel De-Prada-Gil)

validated by means of simulations using MATLAB/Simulink®.

Keywords: Doubly Fed Induction Generator (DFIG), High Voltage Direct Current (HVDC), Offshore Wind Power Plant (OWPP), Variable frequency wind farm, Voltage Source Converter (VSC), Wind power generation

1. Introduction

Offshore wind is a promising energy source which has attracted worldwide attention in recent years as a consequence of various circumstances, such as the lack of available onshore locations (mainly in Europe), the potentially higher and more constant wind speeds at sea than their onshore counterparts (enabling a greater wind power generation) and the fact that space limitations offshore are a less critical issue than inland, which allows the possibility of using larger turbines [1–3].

Thus far, most of the existing offshore wind farms are of a relatively small up to medium sized rating (up to few hundreds MW), and are close enough to the shore that it is feasible transmit the power through HVAC submarine cables [4, 5]. The fact that offshore wind farms are increasingly larger in size and located further away from shore is leading towards the utilization of HVDC technology. Several studies have demonstrated that if the distance between an OWPP and its grid connection point at the Point of Common Coupling (PCC) exceeds a certain critical distance (55-70 km), HVDC transmission becomes the most suitable solution, since it reduces cable energy losses and decreases reactive power requirements [6–8]. There is currently one offshore HVDC project in operation (Bard 1) located about 130 km off the German coast in the North Sea [9].

This trend towards constructing larger wind turbines and locating the offshore wind power plants (OWPPs) increasingly further from shore is posing technical, economic and political challenges that must be overcome to be fully competitive in the long term compared to other types of electricity generation [10, 11]. According to [12], the current Levelised Cost Of Energy (LCOE) for

offshore wind power is estimated to be between 119 and 194 €/MWh, whilst for onshore wind it ranges from 45 and 107 €/MWh. These figures highlights the necessity for cost reduction, which can be achieved, inter alia, through a commitment from government and industry to encourage the development of novel wind power plant designs more cost–effective than the existing ones.

Various researchers propose different innovative concepts in the attempt of cutting down the LCOE. Some of these suggest to extend the DC nature of the high voltage transmission to the collection grid and to consider the possibility of having an entire OWPP in DC [13–15]. Other alternatives aim to consider the offshore collection grid in AC by operating at a non–standard frequency [16]. Likewise, some authors propose a different OWPP topology based on connecting a single large VSC-HVDC converter to the entire AC offshore collection grid (or a wind turbine cluster) which operates at variable frequency [17–24]. Similarly, other studies take advantage of the presence of HVDC technology and its ability to electrically decouple the OWPP from the onshore power system to investigate the dynamic performance of an innovative concept based on a DFIG–based OWPP with reduced power electronic converters connected to a VSC–HVDC converter which operates at variable frequency [25] or at rated V/f operation [26].

This paper deals with the feasibility analysis of this novel concept for OWPPs from the static and dynamic point of view aiming to maximise its energy generation. An optimum electrical frequency search algorithm for the VSC–HVDC converter is proposed and the impact of power converter size of each DFIG–based WT and wind speed variability within the OWPP on the energy yield efficiency, is assessed. Moreover, a coordinated control is implemented between the single large VSC–HVDC converter and all the reduced power converters of each wind turbine. Applying the designed control strategy, the common VSC–HVDC converter provides variable speed control to the WPP by operating it at constant rated V/f [27], while the reduced size power converters inside each DFIG wind turbine are in charge of partially or totally compensating the wind speed difference among turbines due to the wake effect. Consequently, improved

reliability, increased efficiency due to the lower losses and a cost reduction are expected to be achieved, whereas wind energy captured may be reduced owing to the narrower speed range that can be regulated by a smaller power converter.

2. Description of the proposed concept

Fig. 1 shows the proposed wind power plant concept assessed in this paper.

[Figure 1 about here.]

As it can be seen, this wind power plant proposal combines DFIG wind turbines with reduced size power converters (approximately 5–10% instead of 25–35% of the rated power) and a single VSC–HVDC converter which dynamically changes the collection grid frequency (f^*) as a function of the wind speeds of each turbine. This significant reduction of the power converter size is expected to be achieved as a consequence of the variable speed control provided by the common VSC to all the wind turbines. This novel concept requires an HVDC transmission link to decouple the WPP collection grid from the electrical network and it is especially worthwhile for OWPPs where the wind speed variability among turbines is assumed to be lower than in onshore.

The proposed WPP design allows each DFIG–based wind turbine to rotate at different speed within a certain range defined by the size of its partial scale power converter. Thus, depending on the wind speed variability among the wind turbines and the power converter capacity, it is possible to ensure that each wind turbine operates at its optimum point. As an illustrative example, Fig. 2 shows the range of speeds at which all wind turbines can rotate to guarantee its maximum power extraction for a given optimum electrical frequency set by the VSC (f^*=49.3 Hz) and depending on whether the fraction of total power generated by the generator is 30%, 5% or 0% (without converter).

[Figure 2 about here.]

To determine the optimum size of the individual power converters, various criteria such as their capital costs, increased energy capture [28], mechanical

load reduction [29] and Fault Ride Through (FRT) capability [30–34] should be taken into consideration. This paper focuses its study on the energy capture analysis by evaluating in detail the impact of the operating slip admissible range on the aerodynamic losses (or C_P losses) produced by each wind turbine.

This study is addressed by performing two types of analysis with different purposes: firstly, a wind power plant of 12 WTs of 5 MW each is considered to analyze, from a static point of view, the influence of wind speed variability and the power converter size (rated slip) on the energy capture efficiency of this proposed system (i.e., a DFIG-based offshore wind power plant with reduced power converters connected to a single VSC-HVDC operated at variable frequency). This static analysis is offered in Section 3. Secondly, a dynamic analysis is carried out with a case of study consisting of 3 WTs of 1.5 MW each with the aim of both evaluating the feasibility of this proposed concept and understanding the performance of the whole system. This dynamic analysis is shown in Sections 4 and 5.

3. Influence of power converter size and wind speed variability on power generation efficiency

The maximum wind turbine speed range (or slip) that the power converter can regulate is related to the maximum power that can flow (in both directions) through the rotor circuit. This boundary is determined by the voltage upper limit that the power converter can withstand, which sets the power converter size. Thereby, the larger the power converter, the wider the speed range that the generator can regulate, but at a higher cost.

In this section, the impact of the power converter rated slip on energy capture efficiency is analysed. Besides, due to the inherent behaviour of the proposed OWPP concept, in which the electrical frequency within the collection grid is set by the common VSC–HVDC converter according to the individual wind speed of each turbine, the influence of wind speed variability within the OWPP on energy yield efficiency is also investigated.

To this aim, a WPP consisting of 12 wind turbines laid out in a rectangular matrix form of 3 columns and 4 rows is used as a case study (Fig. 4(a)). The rated power of each wind turbine is 5 MW with 126 m of rotor diameter. The spacing between two nearby wind turbines is 7 rotor diameters (D) in the prevailing wind direction and 6 D in its perpendicular wind direction. Regarding the wind conditions within the OWPP, these are defined according to the wind rose and the twelve Weibull distribution functions (one per each wind direction sector considered in the study) presented in Figs. 3(b) and 4(b), respectively. The sets of scale and shape parameters are randomly obtained basing on data reported in [35].

[Figure 3 about here.]

The wind speed of each turbine is obtained for different scenarios by varying the wind direction and the average wind speed of the whole WPP and by assigning to each case its probability of occurrence according to the wind rose and Weibull distribution functions defined above. In order to obtain accurate results, the wake effect within the WPP (single, partial and multiple wakes) is considered. The wind speeds of the upstream wind turbines are randomly generated (for each considered) by means of normal distribution function. This procedure is carried out by using the tool reported in [36], which is based on the methodology detailed in [24]. Once the wind speeds of each WT are known, the optimum electrical frequency, f_e^{opt}, at which the VSC–HVDC converter must operate to maximise the total power generated by the OWPP, is calculated according to the following methodology. To better understand it, the following contents are supported by the two application examples shown in Fig. 4.

1. Given a set of wind speeds, the optimum mechanical speeds at which each wind turbine must rotate to maximise its power output, ω_t^{opt}, are computed. These optimum WT rotational speeds corresponds to the vertical gray lines of Fig. 4.
2. The admissible operational region for all wind turbines is delimited by the size of the converter (lower and upper slip limits) and the minimum and

maximum allowed electrical frequencies within the collection grid (due to the saturation effects of the generators and transformers and field weakening issues, respectively). This region is displayed in blue in Fig. 4 for a particular power converter size with a slip range of ± 5%.

3. The upper and lower frequency limits are defined according to the maximum and minimum values of the optimum wind turbines rotational speeds previously computed in 1) and the maximum slip (s_{max}) of the converter. These limits refer to the two horizontal dashed gray lines of Fig. 4. At this point, two possible scenarios can occur: (i) there is a certain frequency range (for a given power converter size), in which all wind turbines operate at its optimum point, such that the total power generated by the WPP is maximised (Fig. 4(a)). (ii) according to the given slip limits of the converter and the optimum WT speeds of each wind turbine, there is no frequency that maximises the power generated by the whole WPP (Fig. 4(b)). These two situations can be graphically identified by looking at the intersection points between upper and lower slip limits of the converter and minimum and maximum values of the optimum WT speeds, respectively. Thus, scenario (i) is when these intersection points correspond to P1 and P4, whereas scenario (ii) comes about for P2 and P3 intersection points. As it can be seen in Figs. 4(a) and 4(b), these points from P1 to P4 determine the optimum and recommendable operational regions, respectively (green surface), at which the proposed WPP concept must operate to maximise (as much as possible) its power generation.
4. In this last step, the optimum electrical frequency, f_e^{opt}, is calculated for all wind speed sets considered. In case of scenario (i), all the frequency range covered by the optimum operational region are possible to be selected. Thereby, its mean value is chosen as the optimum electrical frequency. With regard to scenario (ii), the more suitable electrical frequency is obtained by undergoing a sweep of N_{freq} electrical frequencies and calculating for each of them the active power generated by the OWPP taking into account the technical constraints of reducing the power converter size.

As a result of the analysis, the frequency that maximises the total power output by the OWPP is chosen. These resulting electrical frequencies refer to the solid violet line of Figs. 4(a) and 4(b), respectively.

[Figure 4 about here.]

In addition, another possible method to find the optimum electrical frequency within the collection grid that maximises the total power generated by the WPP (P^G) is to carry out an optimisation process. In this paper, this mathematical problem is formulated in GAMS as a linear programming (LP) with the following objective function and technical constraints

$$Min \quad (-P^G) \tag{1}$$

s.t.

$$s^{min} \leq s_i \leq s^{max} \qquad \forall i \in \mathcal{I} \tag{2}$$

$$f_e^{min} \leq f_e \leq f_e^{max} \tag{3}$$

where the technical constraints refer to the maximum admissible slip range of the generators and the lower and upper limits of the electrical frequency are defined according to the saturation effects of the generators and transformers and field weakening issues. $\mathcal{I}$ is the set of turbines connected to the single VSC–HVDC converter and P^G can be expressed as

$$P^G = \frac{1}{2}\rho A \sum_{i=1}^{N_{wt}} C_{Pi} v_{wi}^3 \tag{4}$$

$$= \frac{1}{2}\rho A \sum_{i=1}^{N_{wt}} \sum_{j=0}^{N_{pol}} a_j \lambda_i^j v_{wi}^3 \tag{5}$$

where ρ is the air density, $A = \pi R^2$ is the swept area of the wind turbines blades of radius R, v_w is the average wind speed at hub height, N_{wt} is the total number of wind turbines that make up the WPP and C_P is the power coefficient. Thus, in order to linearise the objective function, C_P is approximated to a polynomial of degree N_{pol} and coefficients a_j, which is only dependent on the tip speed ratio λ since the pitch angle β is set to zero to maximise the power output.

Finally, once the optimum electrical frequency is selected and the total power generated by the OWPP is computed, the total energy yield throughout its lifetime, E^G, is obtained as

$$E^G = T \sum_{i=1}^{N_{aws}} \sum_{j=1}^{N_{wd}} P_{ij}^G \; p_{ij}^{wb} \; p_j^{wr}. \tag{6}$$

where T is the lifetime of the offshore installation, N_{aws} and N_{wd} are the number of average wind speeds and wind direction considered, i. e., N_{aws}=30 and N_{wd}=12, and p_{ij}^{wb} and p_j^{wr} are their probability of occurrence, respectively. Notice that both P^G and E^G depend on the collection grid electrical frequency, f_e, and the rated slip of each DFIG converter, s, since they are both function of C_P, which has the following mathematical relation

$$C_P(\lambda) \quad \rightarrow \quad \lambda = \frac{\omega_t R}{v_w} = \frac{2\pi f_e (1-s) R}{p N_{gr} v_w} \tag{7}$$

where ω_t is the wind turbine low speed shaft, p is the pair of poles and N_{gr} is the gearbox ratio. It should be also mentioning that although the average wind speed range considered is from 1 m/s to 30 m/s, only those values greater than the cut–in speed and lower than the cut–out speed are taken into account to compute the total energy yield.

In order to evaluate the influence of the power converter rated slip and the wind speed variability within the OWPP on its energy capture efficiency, the aforementioned methodology has been applied to the case study considering different wind speed standard deviations among the upwind turbines (from 0 to 3 m/s) and different rated slips (0, 5, 15, 30 and 100%). The results are shown in Fig. 5.

[Figure 5 about here.]

As it can be seen, the energy capture efficiency for a power converter rated slip greater than 16.67% is very high even for large wind speed variability within the wind power plant. For instance, the energy yield efficiency of a DFIG–based WPP with a power converter rated slip of 16.67% and 30% is 99.27% and 99.75%, respectively, for a standard deviation among the upstream wind

turbines of 3 m/s. Likewise, it is also noteworthy the better performance of the proposed WPP concept with a reduced power converter rated at 5% of slip compared to the case of generators without any power converter. For example, considering a wind speed standard deviation among the upwind turbines of 1 m/s (a realistic value according to [21]), it improves from 97.21% to 98.52%.

4. Coordinated control scheme

In this section, two different power converter rated slips of 5% and 16.67% for the proposed WPP concept are chosen to be studied in detail. Thus, a comparative energy capture analysis is carried out between them from both the static and dynamic point of view.

In the following, the implemented control system based on a hierarchical structure with both a central control level (VSC–HVDC control system) and a local control level (DFIG wind turbines control system), is presented. This coordinated control is similar to previous DFIG–based WPP control schemes published in [37], but with the peculiarities that in this case there is a central VSC–HVDC large converter that dynamically change the collection grid electrical frequency to maximise the total power generation. In addition, and as a difference with the previous works, the ratings of the power converters of each DFIG wind turbine are reduced, thus curtailing their power control capacity as well.

4.1. System under study

Fig. 6 displays the offshore wind power plant configuration used as a case study. A three pitch–controlled variable–speed 1.5 MW DFIG–based wind turbines connected to a single VSC–HVDC converter, which operates at a constant V/Hz operation has been selected for the validation of the proposed coordinated control concept. Thereby, the central converter changes the voltage with the frequency to maintain the flux constant. The output voltage of each wind turbine is stepped–up from 690 V to 33 kV by a LV/MV transformer. This relatively simple WPP layout facilitates results evaluation. Further, even though such

WPP is not representative of a common offshore one due to the reduced size, it permits to evaluate the effectiveness of optimizing the frequency within the collection grid and to compute the resulting energy yield in a reasonable computational time.

[Figure 6 about here.]

The overall system is modelled using a RMS approach. The model is composed by four main blocks: the VSC–HVDC central control system, the wind speed model, the local control of each wind turbine and the collection grid model. The central control system sets the optimum electrical collection grid frequency according to the wind speeds of each wind turbine, and changes the voltage magnitude at the busbar zero. The wind speed model adopted is explained in detail in [38] and considers mean wind speed component, turbulence as well as rotating sampling effect. The collection grid is represented by the admittance matrix Y and the VSC–HVDC converter (normally based on modular multilevel converter technology [39]) is modeled as a controllable voltage source. In the following, the two control levels are described in more details.

4.2. Wind turbine control

The main control objectives of a wind energy conversion system depends on its load operation mode [37, 40]. In partial load region, which corresponds to wind speeds lower than the rated speed, the aim is to maximize the energy capture from the wind. Otherwise, at hight wind speeds (full load operation mode), the control goal is to limit the generated power below its rated value to avoid overloading.

To achieve these objectives, the control system is divided into two levels (Fig. 7): a high–level control or speed control and a low level control or electrical control. The former gives the proper torque (Γ_m^*), DC voltage (E^*) and reactive powers (Q_s^* and Q_z^*) set points to the converter as function of mechanical rotor angular speed, as well as the frequency and voltage grid. The latter, regulates the incoming reference signals computing the appropriates voltage set points to

the back–to–back power converter. Additionally to this control system, if the machine is operating in the full load region, pitch control is activated in order to keep the extracting power at its nominal value.

[Figure 7 about here.]

The electrical control is divided into two subsystems: the rotor side converter (RSC) control and the grid side converter (GSC) control. Both inner control loops are assumed to be ideal since the WT electric system time responses are much faster than the outer speed control loop or high level control [40]. Thus, it is possible to dissociate both control loops and to define a cascade control structure where the inner control loop concerns the back–to–back power converter and the outer control loop concerns the speed control. Additionally to the the RSC and GSC controls, a DC chopper is implemented in order to dissipate the excess of energy that cannot be evacuated to the grid during a fault. The control system also includes the voltage and currents limitations according to the capacity of the generator and the rating of the converters.

The control scheme implemented for both RSC and GSC is based on the conventional vector control approach [33, 40], but taking into consideration the reduced capabilities of a smaller power converter. Thus, the references voltages that both RSC and GSC must apply to meet their respective control objectives (to regulate the generator torque and the stator reactive power, RSC, and to keep the DC link voltage constant and to control the grid side reactive power, GSC) are limited according to the rated slip chosen for the partial scale frequency converter. This relation between rated slip and maximum rotor voltage allowed is depicted in Fig. 8. Accordingly, the maximum rotor voltage for a power converter sized at 5% of its rated power (case A) is 29.792 V, whereas for a rated slip of 16.67% (case B) it corresponds to 99.326 V.

[Figure 8 about here.]

4.3. VSC–HVDC control system

As previously stated, the VSC–HVDC control system is in charge of controlling its output voltage and the frequency of the collection grid to keep the

flux constant. This V/Hz control method has been widely used due to its easy implementation and good performance [17, 21, 26]. The electrical frequency is dynamically changed by the single converter according to the optimum electrical frequency search algorithm explained in detail in Section 3. This frequency is optimised (f_e^{opt}) based on the wind speed measurements of each wind turbine. In order to maintain the transformer and generator fluxes constant for different electrical frequencies, the output voltage set by the VSC–HVDC power converter located at the offshore platform (V_{VSC}) is computed as

$$V_{VSC} = K f_e^{opt} \tag{8}$$

where K is given by

$$K = \frac{V_{VSC-rated}}{f_{rated}} \tag{9}$$

where $V_{VSC-rated}$ is the rated voltage of the VSC–HVDC converter and f_{rated} is the rated frequency of the grid. Thus,

$$K = \frac{33000}{50} = 660 \tag{10}$$

5. Simulation results: comparative energy capture analysis between a power converter rated slip of 5% and 16.67%

In this section, two dynamic simulations are carried out by using MATLAB /Simulink®. First, a wind speed step change is performed to understand the effect of reducing the power converter rated slip on the overall performance of the system. Then, a scenario with real wind measurements is tested to validate the implemented control scheme, as well as to perform a comparative energy capture analysis between the two power converter sizes considered for the system under study, i.e., 5 % and 16.67 % of rated slip.

5.1. Scenario 1: wind speed step change

Fig. 9 shows the wind speed profile of each wind turbine used for the former simulation. As it can be seen, a wind speed step change occurs at 10 seconds, so that the wind speeds of WT1, WT2 and WT3 before then are 7.5, 7.7 and

7.2 m/s, respectively, while after this time, these wind speeds change to 8.4, 7.9 and 6.6 m/s.

[Figure 9 about here.]

These wind speed values are intentionally chosen to analyse the influence of wind speed variability on the power generation efficiency of the system. As an illustrative example of the performed static analysis, Fig. 10 shows the steady state operational points of the three wind turbines for the two wind speed situations considered (before and after 10 seconds) when the power converted is sized at 5% of rated slip. The vertical gray lines correspond to the optimum rotational speeds of each turbine according to their wind speeds. The horizontal dash black lines represent the resulting optimum electrical frequencies, f_e^{opt}, that must be set by the VSC–HVDC converter to maximise the total OWPP power generation for each case. Thus, it is observed that when all wind speed are similar (Fig. 10(a)), a power converter with a slip range of $\pm 5\%$ is capable enough to carry out the MPPT approach within their limits, so that the OWPP energy capture is maximised. However, if the wind speed variability among turbines increases (Fig. 10(b)), this power converter size is not sufficient to cover this wind speed diversity range (only WT2 is optimised) and to bring each wind turbine speed at its optimum point (C_P^{max}).

[Figure 10 about here.]

The simulation results obtained for both power converter sizes analysed are displayed in Fig. 11.

[Figure 11 about here.]

As it can be noted, before simulation time 10 seconds both OWPP configurations work properly within their limits. Thus, each turbine generates its maximum available wind power, operates at C_P^{max} and rotates at its optimum speed for the given set of wind speeds, since its slip and rotor voltage are within their admissible range. However, after simulation time 10 seconds, the wind speeds

become less uniform between them and the performance of WT1 and WT3 decrease when the rated slip of the converter is 5% (a). Thereby, they cannot rotate at their optimum speed (dash lines) and they generate slightly lower power that could be obtained by a power converter with more capacity (e.g., case (b)) because of their slips and rotor voltages are limited. Notice that this power generation reduction can be clearly observed looking at the steady state C_P values of the three WTs. The maximum admissible voltage is obtained from the rated slip–rotor voltage saturation curve depicted in Fig. 8. It corresponds to case A and B for a power rated slip of 5% or 16.67%, respectively. Accordingly, the rotor voltages required after simulation time 10 seconds for WT1 and WT3 (48.275 V and 72.291 V, respectively) can only be achieved when considering a higher power capacity of the converter (rated slip = 16.67%). Concerning to WT2, the rotor voltage required (14.684 V) is always lower than its upper limit, regardless the rated slip of the power converter. With regard to the electrical frequency imposed by the VSC–HVDC power converter, it matches its reference value (resulted from the static analysis) for both cases considered.

It is worth noting the bidirectional behaviour of the converter according to its slip value. For example, WT1 and WT2 have a negative slip and, therefore, they generated power through the rotor and the stator. However, the positive slip of WT3 means that the rotor is consuming power from the grid, and consequently, it has a negative value.

The results indicate an excellence performance (power efficiency of 99.13%) of the proposed concept by installing smaller power converters inside each DFIG wind turbine. However, it is important remarking that this simulation is based on a wind speed step change, so that a realistic situation considering real time series data is required in order to properly assess both performances in terms of energy capture.

5.2. Scenario 2: wind speed measured data

The second simulation case has as goal to illustrate the overall system performance using a realistic wind speed scenario, as well as to carry out a com-

parative energy capture analysis between the two WPP configurations assessed. Since it is not straightforward to graphically observe any difference between the two cases considered, the presented simulation (Fig. 12) are only referring to the case of a DFIG–based OWPP with reduced converters at 5% of rated slip. Nevertheless, both cases are simulated in order to draw conclusions about their energy capture effectiveness.

In this simulation, the three wind turbines are driven by different turbulent winds, with a time–variant mean speed value obtained from [41] and 5% turbulence intensity. The wind speed profile of each wind turbine, as well as reference frequency that outputs from the central WPP controller and actual frequency set by the VSC–HVDC converter, are depicted in Fig. 12. As it is shown, the reference frequency signal is filtered in order to smooth the effect of operating the collection grid at a variable frequency.

[Figure 12 about here.]

Additionally, the control pitch action is included, since the wind speed data exceed at some points their rated value of 10.1 m/s. The available and actual power generated by the WT3 are also illustrated in Fig. 12 in order to reveal how much energy is curtailed by reducing the power converter at 5% of rated slip. As it can be seen, actual power can achieve its total available power for certain wind speed conditions, whereas in other cases, it is slightly lower.

To quantify the performance of both OWPP configurations considering two different power converter sizes, the energy generated by the three wind turbines throughout the simulation time is calculated and compared with the maximum energy that could be generated for the given wind speed data (by using a full power converter with a rated slip of 100%).

[Table 1 about here.]

As it can be seen in Table 1, the energy yield efficiency when a power converter with a rated slip of 5% and 16.67% is considered account for 98.40% and 99.45%, respectively. These results are consistent with those obtained from the

static analysis (Fig. 5) by assuming that the wind speed data used is fitted as a normal distribution function with a mean value (μ) of 8.6 m/s and a standard deviation (σ) of 0.8 m/s (Fig. 13).

[Figure 13 about here.]

6. Conclusions

This paper proposes an offshore wind power plant configuration arisen thanks to the use of HVDC technology and its ability to allow variable frequency operation within the collection grid. This novel WPP configuration consists of a DFIG–based OWPP with reduced size power electronic converters connected to a single large VSC–HVDC converter which operates at variable frequency within the AC collection grid. Thus, the common VSC–HVDC converter provides variable speed control to the entire wind power plant whilst the reduced size power converters installed inside each DFIG wind turbine aims to compensate (partially or totally) the wind speed difference among turbines due to the wake effect.

The impact of different power converter sizes and wind speed variability within the wind power plant on power generation efficiency is assessed. A coordinated control between the VSC–HVDC converter and the individual back–to–back power converters of each DFIG–based wind turbine is implemented and validated by means of simulations using MATLAB/Simulink®. This control aims to maximise the energy yield by the WPP during its lifetime by optimising the electrical frequency within the collection grid as a function of the wind speed of each turbine. Furthermore, a comparative energy yield analysis between two power converter sizes (with slip ranges of ±5% and ±16.67%) is carried out from the static and dynamic point of view.

The results show a good performance of the proposed system in terms of energy yield efficiency. For example, a power converter with a rated slip of 5% achieves an energy capture efficiency around 98.52% for wind speed standard deviations among the upstream turbines equal or lower than 1 m/s. Also, if

the rated slip of the power converter is reduced by 70% (from 16.67% to 5%), the energy yield efficiency is reduced from 99.45% to 98.40%. Therefore, it can be concluded that the proposed concept, based on DFIG wind turbines and variable frequency operation within the collection grid, could potentially reduce the power converter size, which would imply cost savings. However, since the size of the power converter is not only determined by the maximum slip range allowed, but also by grid integration requirements (e.g., fault ride through capability), this statement must be further analysed in more detail.

Acknowledgements

The research was supported by the EU under the FP7 project IRPWIND and by the Ministerio de Economía y Competitividad, Plan Nacional de I+D+i under Project ENE2012-33043.

[1] J. Wilkes, J. Moccia, Wind in power: 2012 European statistics, Tech. rep., European Wind Energy Association (EWEA) (2013).

[2] B. Möller, L. Hong, R. Lonsing, F. Hvelplund, Evaluation of offshore wind resources by scale of development, Energy 48 (1) (2012) 314–322.

[3] R. Berger, Offshore wind toward 2020. on the pathway to cost competitiveness, Tech. rep., Roland Berger Strategy consultants (April 2013).

[4] X. Sun, D. Huang, G. Wu, The current state of offshore wind energy technology development, Energy 41 (1) (2012) 298–312.

[5] N. Ederer, Evaluating capital and operating cost efficiency of offshore wind farms: A DEA approach, Renewable and Sustainable Energy Reviews 42 (2015) 1034–1046.

[6] N. B. Negra, J. Todorovic, T. Ackermann, Loss evaluation of hvac and hvdc transmission solutions for large offshore wind farms, Electric Power Systems Research 76 (11) (2006) 916–927.

[7] N. M. Kirby, M. J. Luckett, L. Xu, W. Siepmann, HVDC transmission for large off shore wind farms. IEE AC-DC Power Transmission, no. 485, IEE ACDC Power Transmission, London, 2001.

[8] R. L. King, Electrical Transmission systems for large offshore wind farms, Ph.D. thesis, Cardiff University (February 2011).

[9] Bard GroupWebsite 2012, Available: http://www.bard-offshore.de/ (Access data: 22/04/2014).

[10] A. Myhr, and C. Bjerkseter, and A. Ågotnes, and T. A. Nygaard, Levelised cost of energy for offshore floating wind turbines in a life cycle perspective, Renewable Energy 66 (2014) 714–728.

[11] D. E. H. J. Gernaat, and D. P. Van Vuuren, and J. Van Vliet, and P. Sullivan, and D. J. Arent, Global long-term cost dynamics of offshore wind electricity generation, Energy 76 (2014) 663–672.

[12] Levelized cost of electricity renewable energy technologies, Tech. rep., Fraunhofer ISE (November 2013).

[13] N. Holtsmark, H. Bahirat, M. Molinas, B. Mork, H. K. Hoidalen, An All-DC Offshore Wind Farm With Series-Connected Turbines: An Alternative to the Classical Parallel AC Model?, IEEE Transactions on industrial Electronics 60 (2013) 2420–2428.

[14] M. A. Parker, O. Anaya-Lara, Cost and losses associated with offshore wind farm collection networks which centralise the turbine power electronic converters, IET Renewable Power Generation 7 (4) (2013) 390–400.

[15] M. De-Prada-Gil, and J. L. Domínguez-García, and F. Díaz-González, and M. Aragüés-Peñalba, O. Gomis-Bellmunt, Feasibility analysis of offshore wind power plants with DC collection grid, Renewable Energy 78 (2015) 467–477.

[16] J. L. Domínguez-García, D. Rogers, C. Ugalde-Loo, J. Liang, O. Gomis-Bellmunt, Effect of non-standard operating frequencies on the economic cost of offshore AC networks, Renewable Energy 44 (2012) 267–280.

[17] L. Trilla, O. Gomis-Bellmunt, A. Sudrià-Andreu, J. Liang, Control of SCIG wind farm using a single VSC, EPE, 2011, pp. 1–9.

[18] O. Gomis-Bellmunt, A. Junyent-Ferré, A. Sumper, J. Bergas-Jané, Control of a Wind Farm Based on Synchronous Generators With a Central HVDC-VSC Converter, IEEE Transactions on Power Systems 26 (3) (2011) 1632–1640.

[19] D. Jovcic, N. Strachan, Offshore wind farm with centralised power conversion and DC interconnection, IET Generation, Transmission & Distribution 3 (6) (2009) 586–595.

[20] M. de Prada Gil, O. Gomis-Bellmunt, A. Sumper, J. Bergas-Jané, Power generation efficiency analysis of offshore wind farms connected to a SLPC (single large power converter) operated with variable frequencies considering wake effects, Energy 37 (1) (2012) 455–468.

[21] V. Gevorgian, M. Singh, E. Muljadi, Variable Frequency Operations of an Offshore Wind Power Plant with HVDC-VSC, IEEE Power and Energy Society General Meeting San Diego, USA, 2012.

[22] T. Vrionis, X. Koutiva, N. Vovos, G. Giannakopoulos, Control of an HVDC link connecting a wind farm to the grid for fault ride-through enhancement, IEEE Transactions on Power Systems 22 (4) (2007) 2039–2047.

[23] A. Egea-Alvarez, and A. Junyent-Ferré, and J. Bergas-Jané, and F. D. Bianchi, and O. Gomis-Bellmunt, Control of a wind turbine cluster based on squirrel cage induction generators connected to a single VSC power converter, International Journal of Electrical Power and Energy Systems 61 (2014) 523–530.

[24] M. De-Prada-Gil, O. Gomis-Bellmunt, A. Sumper, Technical and economic assessment of offshore wind power plants based on variable frequency operation of clusters with a single power converter, Applied Energy 125 (2014) 218–229.

[25] C. Feltes, I. Erlich, Variable Frequency Operation of DFIG based Wind Farms connected to the Grid through VSC-HVDC Link, in: Power Engineering Society General Meeting, 2007. IEEE, 2007, pp. 1–7.

[26] E. Muljadi, M. Singh, V. Gevorgian, Doubly Fed Induction Generator in an Offshore Wind Power Plant Operated at Rated V/Hz, IEEE Transactions on Industry Applications 49 (5) (2013) 2197–2205.

[27] P. D. C. Perera, F. Blaabjerg, J. K. Pedersen, P. Thogersen, A sensorless, stable V/f control method for permanent-magnet synchronous motor drives, IEEE Transactions on Industry Applications 39 (3) (2003) 783–791.

[28] K. E. Okedu, Impact of Power Converter Size on Variable Speed Wind Turbine, The Pacific Journal of Science and Technology 13 (1) (2012) 176–181.

[29] B. Barahona, N. A. Cutululis, A. D. Hansen, P. Sørensen, Unbalanced voltage faults: the impact on structural loads of doubly fed asynchronous generator wind turbines, Wind Energy.

[30] A. Zohoori, A. Kazemi, R. Shafaie, Fault Ride through Capability Improvement of Wind Turbine Based DFIG Considering an Optimized Crowbar Along with STATCOM under Grid Fault Condition, Research Journal of Applied Sciences, Engineering and Technology 5 (7) (2013) 2297–2302.

[31] A. D. Hansen, G. Michalke, Fault ride-through capability of DFIG wind turbines, Renewable Energy 32 (9) (2007) 1594–1610.

[32] B. Bak-Jensen, T. Kawady, M. H. Abdel-Rahman, Coordination between Fault-Ride-Through Capability and Over-current Protection of DFIG Gen-

erators for Wind Farms, Journal of Energy and Power Engineering 4 (4) (2010) 20–29.

[33] O. Gomis-Bellmunt, A. Junyent-Ferre, A. Sumper, J. Bergas-Jane, Ride-through control of a doubly fed induction generator under unbalanced voltage sags, IEEE Transactions on Energy Conversion 23 (2008) 1036–1045.

[34] A. Luque, and O. Anaya-Lara, and W. Leithead, and G. P. Adam, Coordinated Control for Wind Turbine and VSC-HVDC Transmission to Enhance FRT Capability, Energy Procedia 35 (2013) 69–80.

[35] C. B. Hasager, A. Pena, M. B. Christiansen, P. Astrup, et.al., Remote Sensing Observation Used in Offshore Wind Energy, IEEE Journal of Selected Topics in Applied Earth Observations and Remote Sensing 1 (1) (2008) 67–79.

[36] M. De-Prada-Gil, J. L. Domínguez-García, O. Gomis-Bellmunt, A. Sumper, Technical and economic assessment tool for OWPPs based on a collector grid connected to a single VSC-HVDC converter, EWEC. Barcelona, Spain, 2014.

[37] A. D. Hansen, P. E. Sørensen, F. Iov, F. Blaajberg, Centralised power control of wind farm with doubly fed induction generators , Renewable Energy 32 (7) (2006) 935–951.

[38] F. Díaz-González, A. Sumper, O. Gomis-Bellmunt, R. Villafafila-Robles, A review of energy storage technologies for wind power applications, Renewable and Sustainable Energy Reviews 16 (4) (2012) 2154–2171.

[39] M. Davies, M. Dommaschk, J. Dorn, J. Lang, et.al., HVDC PLUS Basics and Principle of Operation, Tech. rep., Siemens (2008).

[40] R. Pena, J. C. Clare, G. M. Asher, Doubly fed induction generator using back-to-back PWM convertersand its application to variable-speed wind-energy generation, IEE Proceedings Electric Power Applications 143 (3) (1996) 231–241.

[41] National Renewable Energy Laboratory (NREL) webpage, Available: http://www.nrel.gov/ (Access data: 16/03/2014).

List of Figures

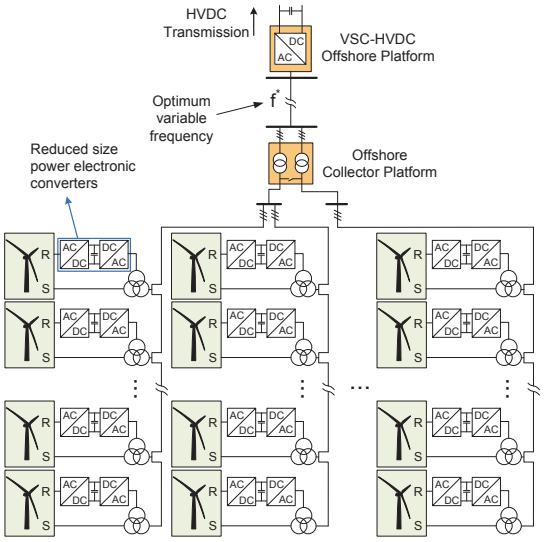

Figure 1: Proposal AC variable frequency OWPP with DFIG wind turbines.

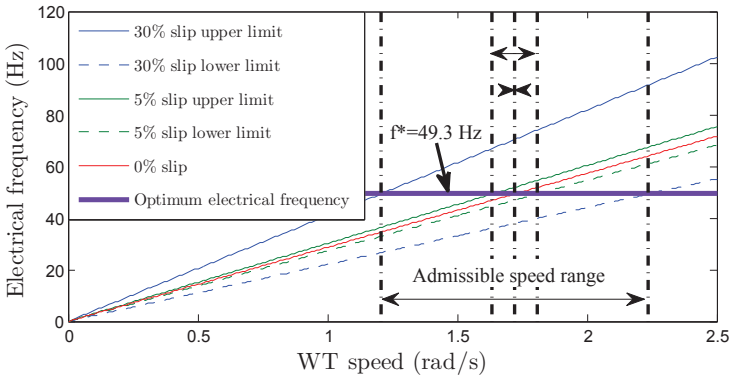

Figure 2: Illustrative example to explain the operation of the proposed WPP concept.

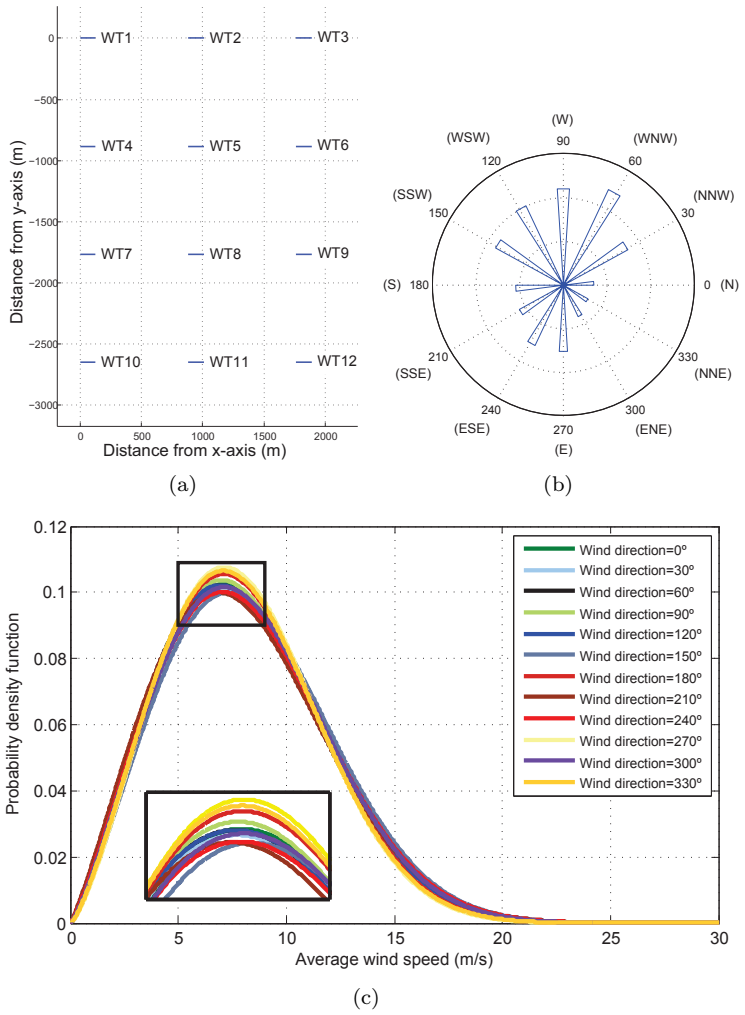

Figure 3: (a) Wind power plant layout (12 wind turbines) considered for the case study. (b) Wind Rose and (c) Weibull (one for each wind direction sector considered) distribution functions at the OWPP location under study.

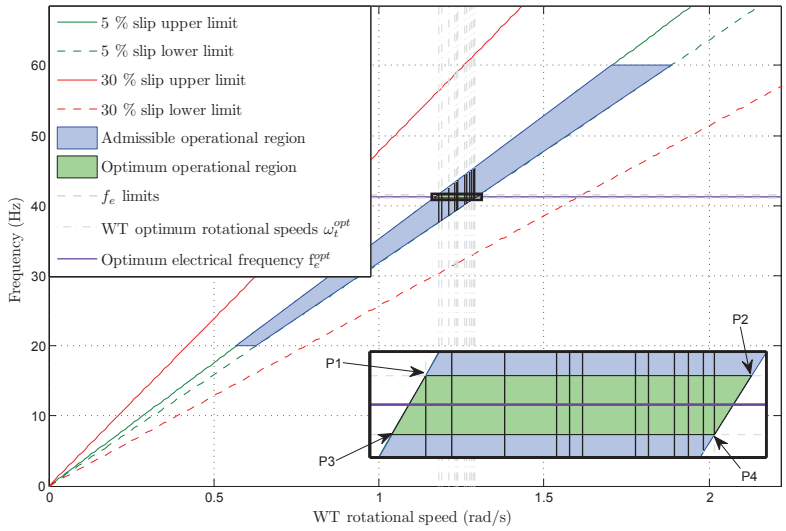

(a)

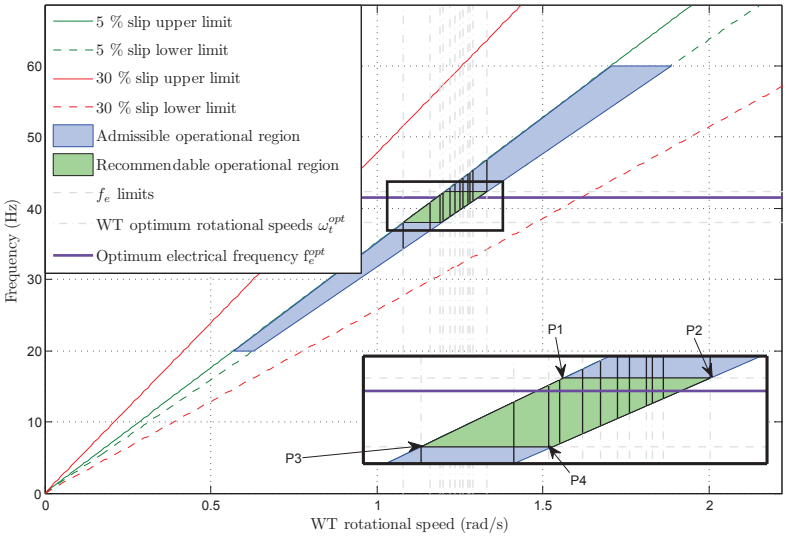

(b)

Figure 4: Two examples of applying the optimum electrical frequency search algorithm for two different sets of wind speeds.

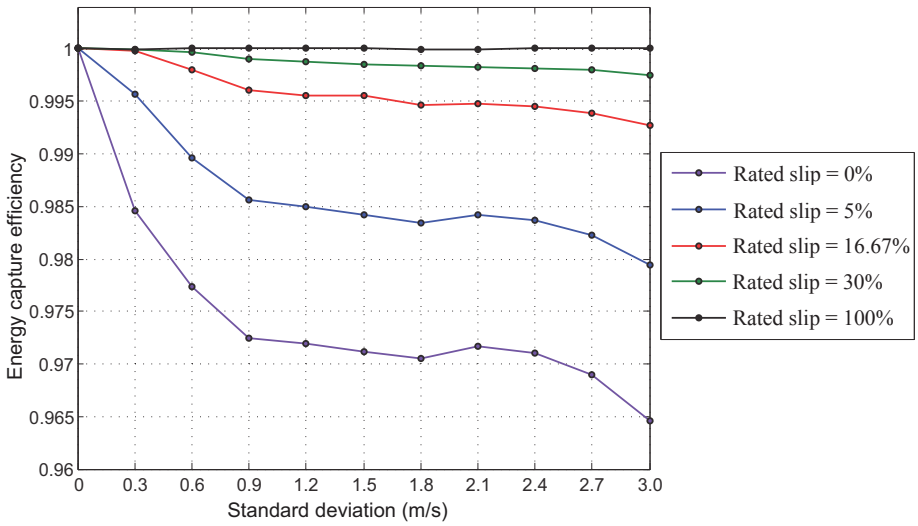

Figure 5: Energy capture efficiency as a function of different wind speed variability within the OWPP and different power converter sizes.

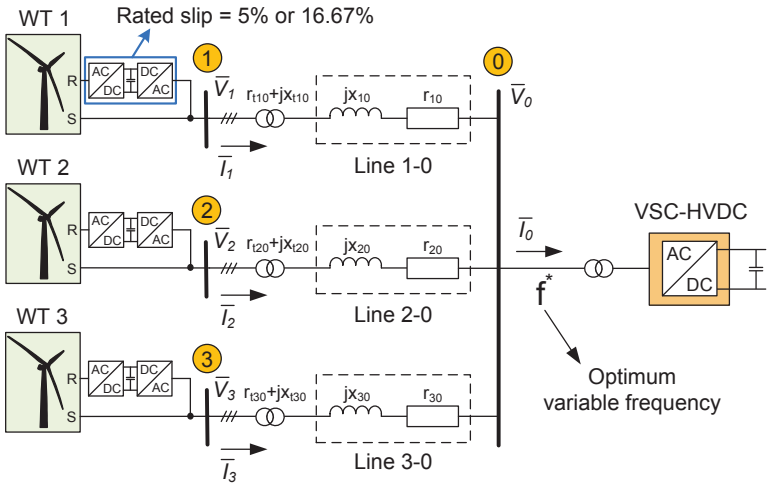

Figure 6: Electrical network topology used for the case study.

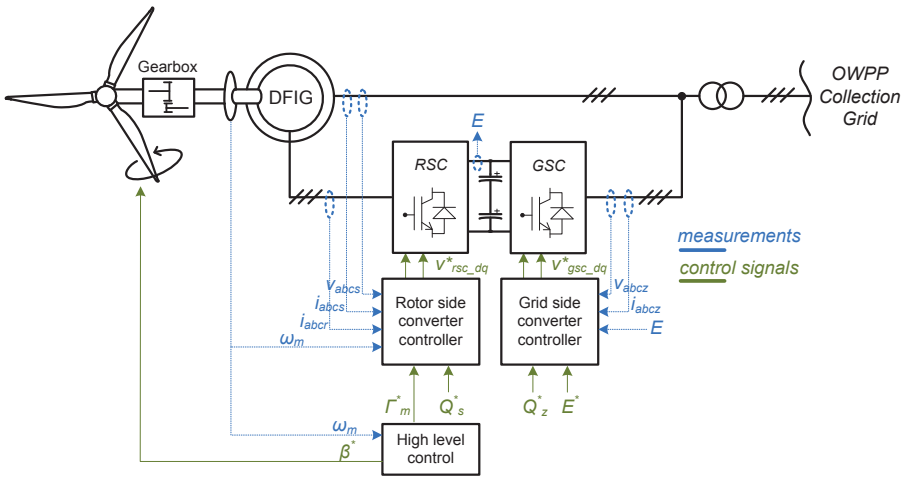

Figure 7: Wind turbine control scheme.

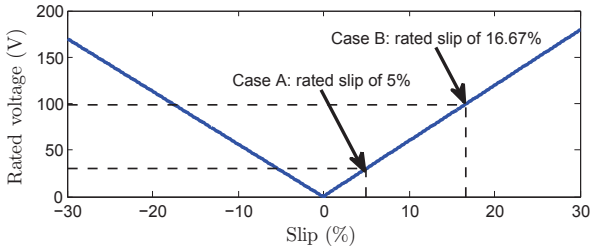

Figure 8: Rated slip - rotor voltage saturation.

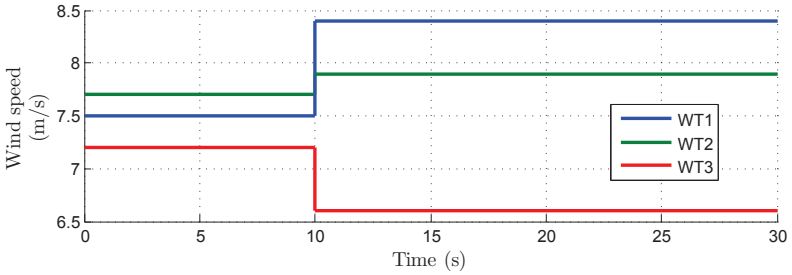

Figure 9: Wind speed profile of each WT considered in scenario 1.

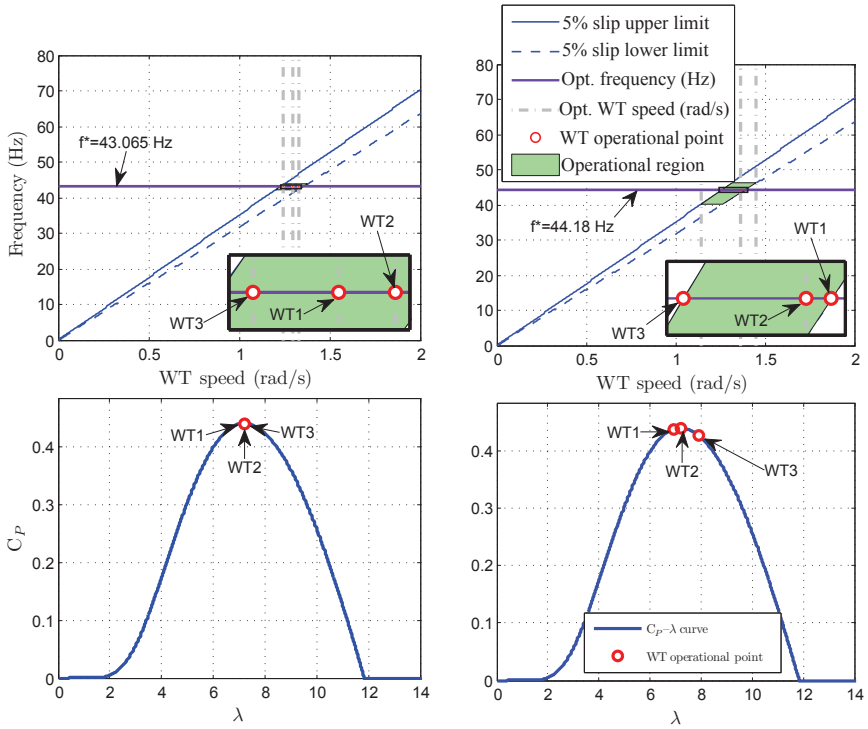

(a) Before t=10 seconds (b) After t=10 seconds

Figure 10: Operational points of WT1, WT2 and WT3 for the two wind speeds situations considered, (a) and (b), when the power converted is sized at 5 % of rated slip.

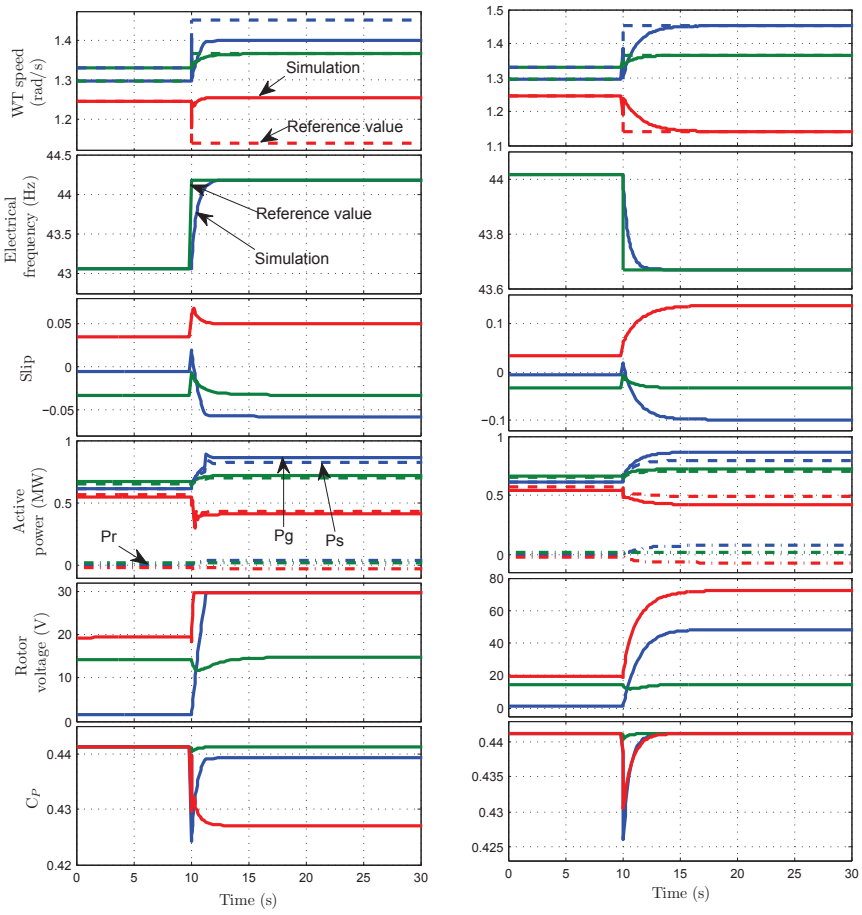

(a) (b)

Figure 11: Simulation results for case 1, considering a power converter rated slip of 5% (a) and 16.67% (b).

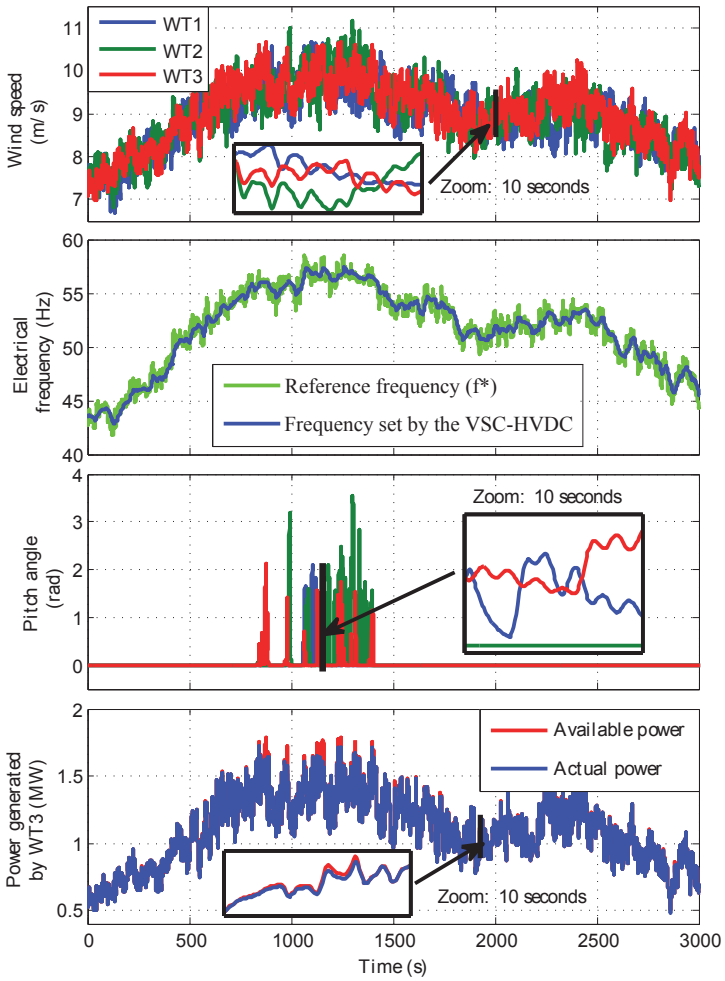

Figure 12: Wind speed data used for scenario 2, frequency set by the VSC–HVDC converter and power generated by WT3 considering a power converter rated slip of 5%.

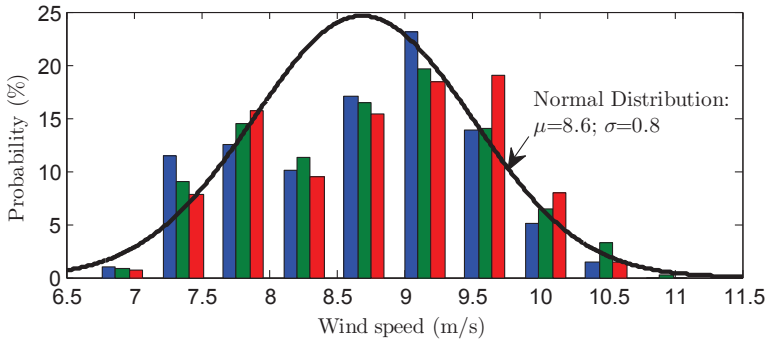

Figure 13: Histogram of the wind speed data used for the study. The solid black line indicates the fitted normal distribution.

List of Tables

Table 1: Comparative energy capture analysis.

Rated	**Energy (MWh)**			**Total**	**Energy yield**
slip (%)	**WT1**	**WT2**	**WT3**	**energy (MWh)**	**efficiency (%)**
5.00	0.9776	1.004	1.0172	2.9988	98.40
16.67	0.9922	1.0104	1.0280	3.0306	99.45
100.00	0.9967	1.0193	1.0315	3.0475	100.00